

Supramolecular Structures Based on New Bolaamphiphile Molecules Investigated by Small Angle and Wide Angle X-ray Scattering and Polarized Optical Microscopy

Mathieu Berchel,^{†,‡} Cristelle Mériadec,^{†,‡} Loïc Lemièvre,^{†,‡} Franck Artzner,^{‡,§} Jelena Jeftić,^{*,†,‡} and Thierry Benvegnu^{†,‡}

UMR CNRS 6226, Sciences Chimiques de Rennes, Equipe Chimie Organique et Supramoléculaire, Ecole Nationale Supérieure de Chimie de Rennes, Avenue du Général Leclerc, CS 50837, 35708 Rennes cedex 7, France, Institut de Physique de Rennes, UMR CNRS 6251, Université Rennes 1, 263, Avenue du Général Leclerc, 35042 Rennes cedex, France, and Université Européenne de Bretagne, 5 boulevard Laënnec, 35000 Rennes, France

Received: April 16, 2009; Revised Manuscript Received: September 18, 2009

In this paper, we present a study of the structural and self-assembling properties of a new family of bolaamphiphiles. These bolaamphiphiles are unsymmetrical, having one sugar polar head at one side and one glycine betaine polar head at the other side. The variations that we introduced concern the length of the main bridging chain that connects the two polar heads as well as the length of the side chain linked at the anomeric position of the sugar moiety. Another variation concerns the introduction of a diacetylenic unit into the main chain in order to rigidify it. We have performed small angle X-ray scattering (SAXS) and wide angle X-ray scattering (WAXS) on the dry compounds as a function of temperature and observed the lamellar structures. We also measured the SAXS and WAXS spectra of aqueous solutions of these compounds that have shown various lamellar structures. The hydrocarbon chain fluidity and, as a consequence, the interlamellar distance varied as a function of temperature. The obtained SAXS and WAXS results are compared with the polarized optical microscopy measurements.

1. Introduction

The small angle X-ray scattering (SAXS) and wide angle X-ray scattering (WAXS) are important techniques to investigate soft matter.¹ For a long time, people used the synchrotron radiation because of its powerful beam,² but today, the SAXS and WAXS facilities are found in more and more laboratories as a tool for everyday use. Very often, the SAXS and WAXS experiments are combined with small angle neutron scattering (SANS) that provides complementary information,^{3,4} especially for biological applications.⁵ The advantage of these techniques is the gain of the insight into the organization of molecules at a large scale, thus enabling investigation of the supramolecular structures and tracking order in apparently disordered systems such as aqueous solutions of amphiphiles⁶ or proteins,⁷ biologically active molecules,⁸ and other systems.^{9,10}

In the last few decades, much research has been done in order to formulate and characterize complex lyotropic liquid crystalline phases (lamellar, hexagonal, and cubic structures) of amphiphilic lipids and their aqueous nanostructured dispersions.^{11–16} These systems are important in both scientific and industrial fields. Self-assembled structures of lipids build up biological membranes, and they play an important role in cell structure and functions.¹⁷ Many practical applications of these systems have been reported,^{18–22} and they remain of important current interest in membrane dynamics and its functions.^{23–27} Caffrey and co-workers have studied the rich polymorphism of binary monoglyceride/water phases in detail: these systems display, in general, a variety of assemblies, depending on

concentration and temperature.^{28–31} Such phase diagrams often feature different phases: an isotropic phase (L or I), a fluid lamellar phase (L_a), a tilted lamellar phase (L_β'), an inverted type of hexagonal phase (H_2), an inverted bicontinuous cubic (V_2) liquid crystalline phase, at low temperature a lamellar crystalline phase (L_c), and others. To better design the new lipid systems in the future, it is important to understand the nanostructural arrangement that significantly affects the delivery properties of the system, as well as its other properties. Gruner and co-workers³² have investigated the thermotropic phase behavior of the diastereomeric ditetradecyl- β -D-galactosyl glycerols and their mixture, and X-ray diffraction measurements identify the phase transitions as the L_β (or L_β')/ L_a and L_a/H_2 phase transitions. They studied some interesting aspects of the properties of asymmetric chain phosphatidylcholines that form mixed interdigitated gel phases.³³ Mannock and McElhaney³⁴ have studied the thermotropic properties of a homologous series of saturated, synthetic β -D-galactosyl diacylglycerols varying in their hydrocarbon chain length. Hinz and co-workers studied the polymorphism of synthetic 1,2-dialkyl-3-O-beta-D-galactosyl-sn-glycerols of different alkyl chain lengths.³⁵ In our work, we present a study of the phase diagram by SAXS/WAXS and polarized optical microscopy of a new family of so-called bolaamphiphile molecules where we varied the chain length of the main bridging chain and of the side chain, and introduced a diacetylenic unit in some cases in order to rigidify the structure.

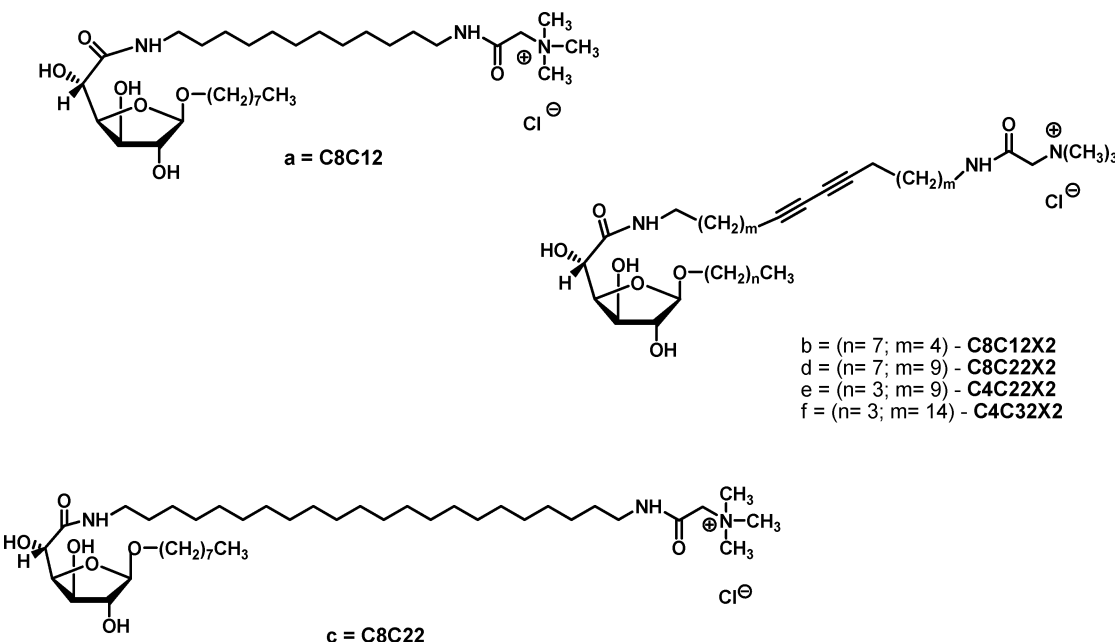
One class of amphiphiles, the so-called bolaamphiphiles bearing two polar head groups on two opposite sides of the main bridging hydrocarbon chain can have one or more side chains.³⁶ These molecules appear in nature as archaeal lipids³⁷ and are interesting as drug delivery vectors.³⁸ Very important work on the chemical structure and physical polymorphism of different lipidic components of archaeabacteria has been reported

* Corresponding author. E-mail: jelena.jeftic@ensc-rennes.fr. Phone: +33 2 23 23 80 34. Fax: +33 2 23 23 80 46.

[†] Ecole Nationale Supérieure de Chimie de Rennes.

[‡] Université Européenne de Bretagne.

[§] Université Rennes 1.

SCHEME 1: Compounds Characterized and Analyzed in This Paper

by A. Gulik, V. Luzzati, M. De Rosa, and A. Gambacorta in refs 39–41. As Archaea are the organisms that survive in harsh environments such as high salinity, high acidity, very high or very low temperature, or high pressure, the scientists are interested in mimicking the synthesis of archaeolipids in order to produce sufficiently stable vectors for drug delivery.^{42–44} The organization of bolaamphiphilic lipids in aqueous solutions can be quite complex and is widely described in the literature for various systems.^{45–50} The need to synthesize new, even more efficient bolaamphiphile molecules and to determine their structures is however growing because of these important applications.

In the present paper, we study a family of bolaamphiphiles bearing one sugar polar headgroup and one glycine betaine polar headgroup interconnected with a main bridging hydrocarbon chain and possessing a side chain linked at the anomeric site of the sugar moiety. We synthesized bolaamphiphile molecules with different lengths of the main hydrocarbon chain, and in order to modulate the hydrophilic/lipophilic balance, we modified the length of the side carbon chain as well. Willingly to observe the influence on the membrane fluidity of the supramolecular structures, made out of these bolaamphiphilic molecules, we introduced the diacetylenic unit into the main hydrocarbon chain to rigidify the molecule. The main technique that we used to explore these properties is small angle and wide angle X-ray scattering, equipped with a thermal control. Indeed, we could point out the lamellar properties of these dry molecules also upon dispersing them in water. The synthesis of unsymmetrical saturated or diacetylenic cationic bolaamphiphiles has been reported previously where we started to investigate the self-assembling properties of bolaamphiphile molecules by using the cryo-TEM (transmission electron microscopy) technique.⁵¹ It provided answers to some of the open questions, that is, the three-dimensional organization, but the question of whether the molecules are organized in symmetrical or unsymmetrical monolayers, bilayers, or mixed systems still remained unresolved. The appropriate technique to approach this question is the small angle X-ray scattering and wide angle X-ray scattering. We now report full experimental details on SAXS/WAXS measurements of these original bolalipids containing one

glycosidic residue based on D-glucuronolactone and one cationic glycine betaine moiety, as polar heads.

2. Experimental Section

2.1. Materials. Preparation of Bolaamphiphiles. General (see Scheme 1). All commercially available chemicals were used without further purification, and solvents were carefully dried and distilled prior to use. Unless otherwise noted, nonaqueous reactions were carried out under a nitrogen atmosphere. Analytical TLC was performed on Merck 60 F254 silica gel nonactivated plates. A solution of 5% H₂SO₄ in EtOH was used to develop the plates. Merck 60 H (5–40 μm) silica gel was used for column chromatography. ¹H and ¹³C NMR spectra were recorded at 400 and 100 MHz, respectively. Furanoside derivatives were numbered as for the systematic nomenclature for the assignments of ¹H and ¹³C NMR data. NMR spectra in CDCl₃/CD₃OD were calibrated from the residual CHCl₃ signal. Fast-atom bombardment (FAB) mass spectra were acquired on a MS/MS TOF mass spectrometer with *m*-nitrobenzylic alcohol as the matrix.

The procedure of preparation is the same as reported in refs 51 and 52, and here, we give the characterization of products not described before. The abbreviations used here for different molecules indicate the number of carbon atoms in the side chain and the number of atoms in the main chain as well as the presence or the absence of the conjugated triple bonds. Thus, molecule **a** contains 8 carbon atoms in the side chain and 12 carbon atoms in the main chain (C8C12) and molecule **b** contains the diacetylenic unit in addition designated by X2 (C8C12X2).

All of the aqueous solutions of bolaamphiphiles were prepared by introducing a small amount (up to 2 mg) of the compound into a glass capillary for X-ray measurements of 1.5 mm diameter and then diluted with 10–20 μL of distilled water. To homogenize the solution, we stirred it with a metal needle. We used this mechanical way of mixing in order to not thermally influence the sample. The measured solutions were homogeneous. In the case where the precipitation took place after several days, we put the capillaries at 40 °C for 1 h and cooled them

back to room temperature over 1 day. The subsequent spectra were equivalent to the initial spectra.

The dry samples were prepared by freeze-drying and kept in the refrigerator prior to use. They were thermally equilibrated overnight at room temperature and for 1 h at each given temperature to record the spectra.

The temperature has been calibrated with a thermocouple at the position of the capillary bottom. After reaching the assigned temperature, the acquisition time for one spectrum is over 1 h to ensure the sample thermal equilibrium. We have performed several experiments for one series of temperatures and have obtained reproducible results. The temperature precision is ± 0.4 °C.

Chemical Characterization of Bolaamphiphiles b (C8C12X2), c (C8C22), d (C8C22X2), e (C4C22X2), and f (C8C32X2). *N-(12-Betainylamino-dodeca-5,7-diynyl)-octyl β-D-Glucofuranosiduronamide Chloride:* b (C8C12X2). *Rf* [EtOAc/iPrOH/H₂O: 6:3:1]: 0.2. $[\alpha]^{20}_D$: -20.3° (c 1.0, MeOH). IR ν (cm⁻¹) (nujol): 3365 (O—H), 1650 (C=O). Mp: 65 °C. ¹H NMR (CD₃OD, 400 MHz) δ (ppm): 0.87 (CH₃(CH₂)₇O, t, 3H, J = 7.0 Hz), 1.27–1.37 (CH₂, m, 10H), 1.50–1.63 (CH₂, m, 10H), 2.27 (CH₂C≡C, t, 4H; J = 6.9 Hz), 3.16 (NHCH₂, m, 2H), 3.25 (NHCH₂, m, 2H), 3.29 (N⁺(CH₃)₃, s, 9H), 3.34 (OCH₂, dt, 1H, J = 6.7, 9.4 Hz), 3.74 (OCH₂, dt, 1H, J = 6.7, 9.4 Hz), 3.97 (s, 1H²), 4.05 (dd, 1H³, J = 1.6, 4.7 Hz), 4.10 (N⁺CH₂CO, s, 2H), 4.32 (d, 1H⁵, J = 5.4 Hz), 4.36 (t, 1H⁴, J = 5.0 Hz), 4.83 (s, 1H¹). ¹³C NMR (CD₃OD, 100 MHz) δ (ppm): 14.9 (CH₃(CH₂)₇O), 19.77, 19.83, 24.2, 27.16, 27.20, 27.7, 29.7, 30.0, 30.9, 31.03, 31.05, 33.5 (CH₂), 39.9 (CH₂NH), 40.3 (NHCH₂), 55.2 (N⁺(CH₃)₃), 66.2 (N⁺CH₂CO), 67.0, 67.2 (CH₂C≡C), 70.0 (OCH₂), 72.5 (C⁵), 77.86, 77.95 (CH₂C≡C), 78.2 (C³), 82.2 (C²), 84.4 (C⁴), 110.4 (C¹), 165.1 (N⁺CH₂CO), 175.1 (C=O). HRMS (LSIMS, Cs⁺, mNBA): calcd for C₃₁H₅₄N₃O₇, 580.3916; found, 580.3972.

N-(22-Betainylamino-docosane)-octyl β-D-Glucofuranosiduronamide Chloride: c (C8C22). *Rf* [EtOAc/iPrOH/H₂O: 6:3:1]: 0.2. IR ν (cm⁻¹) (nujol): 3365 (O—H), 1650 (C=O). Mp: 113 °C. ¹H NMR (CD₃OD, 400 MHz) δ (ppm): 1.05 (CH₃(CH₂)₇O, t, 3H, J = 7.0 Hz), 1.44–1.77 (CH₂, m, 44H), 1.41–1.54 (CH₂, m, 8H), 3.35 (CH₂NH, m, 2H), 3.40 (NHCH₂, m, 2H), 3.49 (N⁺(CH₃)₃, s, 9H), 3.55 (OCH₂, dt, 1H, J = 6.7, 9.4 Hz), 3.88 (OCH₂, dt, 1H, J = 6.7, 9.4 Hz), 4.16 (s, 1H²), 4.24 (dd, 1H³, J = 1.6, 4.7 Hz), 4.27 (N⁺CH₂CO, s, 2H), 4.51 (d, 1H⁵, J = 5.4 Hz), 4.54 (t, 1H⁴, J = 5.0 Hz), 5.01 (s, 1H¹). ¹³C NMR (CD₃OD, 100 MHz) δ (ppm): 14.5 (CH₃(CH₂)₇O), 23.8, 27.3, 28.1 (2C), 30.2, 30.46, 30.53, 30.55, 30.58, 30.68, 30.70, 30.76, 30.83 (13C), 33.1 (CH₂), 40.3 (CH₂NH), 40.6 (NHCH₂), 55.0 (N⁺(CH₃)₃), 65.8 (N⁺CH₂CO), 69.6 (OCH₂), 72.2 (C⁵), 77.7 (C³), 81.9 (C²), 84.1 (C⁴), 110.1 (C¹), 164.6 (N⁺CH₂CO), 174.5 (C=O). HRMS (LSIMS) (Cs⁺, mNBA): calcd for C₄₁H₇₄N₃O₇ [M]⁺, 720.5527; found, 720.5528.

N-(22-Betainylamino-docosa-10,12-diynyl)-octyl β-D-Glucofuranosiduronamide Chloride: d (C8C22X2). *Rf* [EtOAc/iPrOH/H₂O: 6:3:1]: 0.2. IR ν (cm⁻¹) (nujol): 3365 (O—H), 1650 (C=O). $[\alpha]^{20}_D$: -24.6° (c 1.0, MeOH). Mp: 80–85 °C. ¹H NMR (CD₃OD, 400 MHz) δ (ppm): 0.85 (CH₃(CH₂)₇O, t, 3H, J = 7.0 Hz), 1.25–1.38 (CH₂, m, 20H), 1.45–1.47 (CH₂, m, 12H), 2.19 (CH₂C≡C, t, 4H, J = 6.9 Hz), 3.16 (NHCH₂, m, 2H), 3.25 (NHCH₂, m, 2H), 3.26 (N⁺(CH₃)₃, s, 9H), 3.34 (OCH₂, dt, 1H, J = 6.7, 9.4 Hz), 3.69 (OCH₂, dt, 1H, J = 6.7, 9.4 Hz), 3.94 (s, 1H²), 4.02 (dd, 1H³, J = 4.7 Hz), 4.08 (N⁺CH₂CO, s, 2H), 4.29 (d, 1H⁵, J = 5.4 Hz), 4.36 (t, 1H⁴, J = 5.0 Hz), 4.79 (s, 1H¹). ¹³C NMR (CD₃OD, 100 MHz) δ (ppm): 14.6 (CH₃(CH₂)₇O), 19.7 (2C), 23.8, 27.3 (2C), 28.0, 29.6 (2C), 29.90, 29.92, 30.16

(2C), 30.19, 30.34, 30.46, 30.50, 30.54, 30.56, 30.63, 30.67, 30.69, 33.1 (CH₂), 40.3 (CH₂NH), 40.6 (NHCH₂), 54.8 (N⁺(CH₃)₃), 65.9 (N⁺CH₂CO), 66.5 (CH₂C≡C), 69.5 (OCH₂), 72.2 (C⁵), 77.6 (C³), 77.9 (CH₂C≡C), 81.9 (C²), 84.2 (C⁴), 110.0 (C¹), 164.8 (N⁺CH₂CO), 174.5 (C=O). HRMS (ESI+): calcd for C₄₁H₈₂N₃O₇ [M]⁺, 728.6153; found, 728.6152.

N-(22-Betainylamino-docosa-10,12-diynyl)-butyl β-D-Glucofuranosiduronamide Chloride: e (C4C22X2). *Rf* [EtOAc/iPrOH/H₂O: 6:3:1]: 0.2. IR ν (cm⁻¹) (nujol): (CO) 1650; (OH) 3365. $[\alpha]^{20}_D$: -46° (c 1.0, MeOH). Mp: 80–85 °C. ¹H NMR (CD₃OD, 400 MHz) δ (ppm): 0.92 (CH₃(CH₂)₃O, t, 3H, J = 7.0 Hz), 1.25–1.38 (CH₂, m, 28H), 1.45–1.47 (CH₂, m, 12H), 2.22 (CH₂C≡C, t, 4H; J = 6.9 Hz), 3.20 (NHCH₂, m, 2H), 3.23 (NHCH₂, m, 2H), 3.30 (N⁺(CH₃)₃, s, 9H), 3.43 (OCH₂, dt, 1H, J = 6.7, 9.4 Hz), 3.68 (OCH₂, dt, 1H, J = 6.7, 9.4 Hz), 3.98 (s, 1H²), 4.07 (dd, 1H³, J = 1.6, 4.7 Hz), 4.10 (N⁺CH₂CO, s, 2H), 4.34 (d, 1H⁵, J = 5.4 Hz), 4.39 (t, 1H⁴, J = 5.0 Hz), 4.80 (s, 1H¹). ¹³C NMR (CD₃OD, 100 MHz) δ (ppm): 14.1 (CH₃(CH₂)₃O), 19.7 (2C), 20.4, 27.97, 27.99, 29.5 (2C), 29.9 (2C), 30.1 (2C), 30.3, 30.42, 30.47, 30.53, 30.58, 32.8, 34.3 (CH₂), 40.0 (CH₂NH), 40.3 (NHCH₂), 54.6 (N⁺(CH₃)₃), 65.6 (N⁺CH₂CO), 66.2 (CH₂C≡C), 69.1 (OCH₂), 72.0 (C⁵), 77.53 (C³), 77.7 (CH₂C≡C), 81.6 (C²), 83.8 (C⁴), 109.8 (C¹), 164.4 (N⁺CH₂CO), 174.5 (C=O).

N-(32-Betainylamino-dotriaconta-15,17-diynyl)-butyl β-D-Glucofuranosiduronamide Chloride: f (C4C32X2). *Rf* [EtOAc/iPrOH/H₂O: 6:3:1]: 0.1. ¹H NMR (CD₃OD, 400 MHz) δ (ppm): 0.91 (CH₃(CH₂)₃O, t, 3H, J = 7.0 Hz), 1.28–1.40 (CH₂, m, 40H), 1.44–1.56 (CH₂, m, 12H), 2.22 (CH₂C≡C, t, 4H, J = 6.9 Hz), 3.19 (NHCH₂, m, 2H), 3.23 (NHCH₂, m, 2H), 3.30 (N⁺(CH₃)₃, s, 9H), 3.38 (OCH₂, dt, 2H, J = 6.7, 9.4 Hz), 3.97 (H², s, 1H), 4.05 (H³, dd, 1H, J = 4.8, 1.7 Hz), 4.08 (⁺NCH₂CO, s, 2H), 4.26 (H⁵, d, 1H, J = 5.4 Hz), 4.38 (H⁴, t, 1H, J = 5.0 Hz), 4.81 (H¹, s, 1H). ¹³C NMR (CD₃OD, 100 MHz) δ (ppm): 14.4 (CH₃(CH₂)₃O), 19.7 (2C), 20.4, 29.6 (2C), 29.9 (2C), 30.2 (3C), 30.4, 30.51, 30.54, 30.65 (2C), 30.73 (2C), 30.77 (3C), 30.81 (2C), 30.83, 32.8, 34.3 (CH₂), 40.3 (CH₂NH), 40.6 (NHCH₂), 54.8 (N⁺(CH₃)₃), 65.8 (N⁺CH₂CO), 66.5 (CH₂C≡C), 69.2 (OCH₂), 72.3 (C⁵), 77.6 (C³), 77.9 (CH₂C≡C), 81.8 (C²), 84.1 (C⁴), 110.0 (C¹), 164.6 (⁺NCH₂CO), 174.5 (C=O). HRMS (ESI+): calcd for C₄₇H₈₆N₃O₇ [M]⁺, 804.6466; found, 804.6468.

2.2. Methods. **2.2.1. Small and Wide Angle X-ray Scattering (SAXS/WAXS).** *X-ray Diffraction.* X-ray scattering experiments were performed using a FR591 Bruker AXS rotating anode X-ray generator operated at 50 kV and 50 mA with monochromatic Cu K α radiation (λ = 1.541 Å) and point collimation. X-ray patterns were collected with a Mar345 Image-Plate detector (Marresearch, Norderstedt, Germany). The monochromatic Cu K α radiation (λ = 1.541 Å) was directed with a 350 μm × 350 μm focal spot at 320 mm by a double reflection on an elliptic cross multilayer Montel mirror (Incoatec, Geesthacht, Germany). The beam was defined under vacuum by four motorized carbon–tungsten slits (JJ-Xray, Roskilde, Denmark) positioned in front of the mirror (500 μm × 500 μm). Four additional guard slits (600 μm × 600 μm) were placed at the focal point with a 220 mm slit separation distance. The flux after the output mica windows was 3×10^8 photons/s. A 2 mm diameter square lead beam stop was placed under a vacuum at 270 mm; afterward, the sample and the detector were positioned at 420 mm. The X-ray patterns were therefore recorded for a range of reciprocal spacing $q = 4\pi \sin \theta/\lambda$ from 0.03 to 1.6 Å⁻¹, where θ is the diffraction angle. The repetition distances $d = 2\pi/q$ should be between 200 and 3.9 Å. The samples were

placed into 1.5 mm glass capillaries (Glas W.Müller, Germany) and introduced into a homemade capillary holder, which can maintain up to 20 capillaries at a controlled temperature. We use the programs *Fit 2D* and *IgorPro* to treat the data.⁵³

2.2.2. Polarized Optical Microscopy. Phase identification was carried out using a Leika DMLS polarizing microscope equipped with the Sony Sc-DC 38P digital camera. Studies on the lyotropic behavior of the compounds were carried out by placing a small amount (~ 10 mg) of each material on a microscope slide, covering it with a coverslip, and then inserting water under the coverslip. The water diffusion generated a concentration gradient starting from dilute aqueous solution to the neat material. The mesophases were all classified via examination of the defect textures formed in the polarized transmitted light microscope.⁵⁴

3. Results

3.1. Small Angle X-ray Scattering. **3.1.1. Operational Definitions of the Different “Phases”— L_α , L_β' , L_c , L , and I —and Nanotubes That Are Further Mentioned.** Lipid bilayers are the most frequent structures formed by lipids, as they are present in every cellular organism.¹¹ A planar lipid membrane typically occurs for lipids with a packing parameter close to 1, which means that an individual lipid molecule fits to a cylinder. The vast majority of bilayers in a biological context has an asymmetry—the interior and exterior of the cellular compartment—resulting in a finite spontaneous curvature. However, recent studies by small-angle X-ray and neutron scattering showed that the inner and outer leaflets of vesicle bilayers can be indistinguishable, even for highly curved vesicles with diameters down to 62 nm.⁵⁵

Several bilayers can pile up with a thin layer of water solution separating each of them. According to its state, a lipid bilayer is said to be in the L_α liquid crystalline phase when it is fluid with melted hydrocarbon chains and in the L_β' tilted phase when the gel phase, below the phase transition temperature, tilts relative to the layer normal. We can call L_α and L_β' the liquid disordered and liquid ordered lamellar phases, respectively. These phases are quite common with phosphatidylcholine (PC) lipids.⁵⁶ In the small angle region, one observes a sharp peak with its harmonics in a pattern of 1:2:3:4. In the wide angle region, there are no sharp peaks present for the phase L_α , while for the phase L_β' there is one typical peak, helping us to distinguish these two phases.

The crystalline lamellar structure, L_c , consists of piles of bilayers, but in this structure, the molecules are no more fluid which results in many sharp peaks in the wide angle region upon X-ray scattering, being the fingerprint of this phase.

The lamellar isotropic L structure consists of short parts of lamellae (or bilayers) that are distributed in a random way resulting in a large polydisperse signal in a small angle region. For the aqueous solution, the same type of signal is a result of the random distribution of short parts of bilayers dispersed statistically in water. This phase is called an isotropic liquid, I phase. One interesting study of self-assembly of flat nanodiscs in salt-free catanionic surfactant solutions has been reported.⁵⁷ The authors observe the nanodiscs coexistent with a lamellar structure.

Finally, lipid nanotubes consist of multiple lipid bilayers rolled up in a long cylinder.^{58,59} Their inner diameter ranges from ~ 10 nm with synthetic lipids to hundreds of nanometers for natural phospholipids, and their length can reach up to several centimeters.⁶⁰

3.1.2. Analysis of the Spectra of Dry Compounds: C8C12 (a), C8C12X2 (b), C8C22 (c), C8C22X2 (d), C4C22X2 (e),

C4C32X2 (f). The first series of investigation has been performed on dry samples of the family of compounds: C8C12 (a), C8C12X2 (b), C8C22 (c), C8C22X2 (d), C4C22X2 (e), and C4C32X2 (f) (see Scheme 1). We have studied by small and wide angle X-ray scattering (SAXS/WAXS) the thermal dependence of these compounds upon heating in the range of temperatures between 23 and 70 °C in intervals of 10 °C and then cooling back to ambient temperature (a.t.). All of the samples were kept at a given temperature for 1 h for each spectrum to ensure the thermal equilibration. Generally, the behavior of these samples is liquid crystalline thermotropic because their structure depends on the temperature changes. In Figures 1a–1f, we see the thermal dependence of SAXS/WAXS spectra of these six dry compounds.

The compound **C8C12** presents the lamellar crystalline phase L_c at 23 and 30 °C (Figure 1a) as we can see from the wide angle X-ray scattering (WAXS) region where many sharp peaks are present. The first peak in the small angle region is placed at 0.24 Å⁻¹ which corresponds to an interlamellar distance of 26.2 Å at 23 °C. By heating up to 40 °C, we see that sharp peaks in the wide angle region disappear. The main peak, which is shifted toward wider angles to 0.26 Å⁻¹, and its two harmonics at 0.51 and 0.71 Å⁻¹ correspond to the pattern 1:2:3. Therefore, we conclude that the compound changes its structure to the lamellar L_α phase that remains present up to 70 °C. Upon heating up to 70 °C, one observes the shift of the main peak and its harmonics toward the wide angles (smaller distances). This is interpreted as if the chains become more and more flexible by increasing the temperature. The polar heads of one and the same bolaamphiphile molecule are less distanced, which results in shorter lamellar layers. By cooling back down to ambient temperature, the same hydrocarbon chains are less flexible, and in consequence, the distance between the layers becomes larger. The system remains in the lamellar alpha (L_α) phase (Scheme 2a).

In Table 1, the interlayer distances are listed for the range of temperatures between 23 and 70 °C for all six dry compounds.

The first chemical change that we introduced was to insert a diacetylenic unit in the middle of the main (bridging) hydrocarbon chain. The SAXS/WAXS spectra of this compound C8C12X2 are shown in Figure 1b. They represent one large peak that shifts toward wide angles (shorter distances) by increasing the temperature. This large peak is a result of the polydisperse signal on shorter lamellae that are distributed in a random way which is a signature for the isotropic lamellar L phase.

A further chemical challenge was to compare the influence of the main chain length on the supramolecular organization. Therefore, we have synthesized the compound **C8C22** with 22 methylene units in the main (bridging) chain and we kept the length of 8 methylene units in the side chain. In the series of spectra in Figure 1c for the spectrum at 23 °C, we observe one main peak at 0.17 Å⁻¹ with three of its harmonics corresponding to a 1:2:3:4 pattern. In addition, we observe in the wide angle region a peak at 1.48 Å⁻¹ which is a typical signature of the lamellar L_β' phase (Scheme 2b) where the molecules are tilted corresponding to the axis perpendicular to the lamellar surface.^{61–63} One observes a shift of the main peak and its harmonics toward wide angles, that corresponds to shorter distances, by increasing the temperature from 23 to 40 °C. This again means that the interlamellar distances shorten upon increasing the temperature because of the fluidity of the chains.⁶² By increasing the temperature to 50 °C, all narrow peaks disappear and the conclusion is that the L_β' lamellar phase

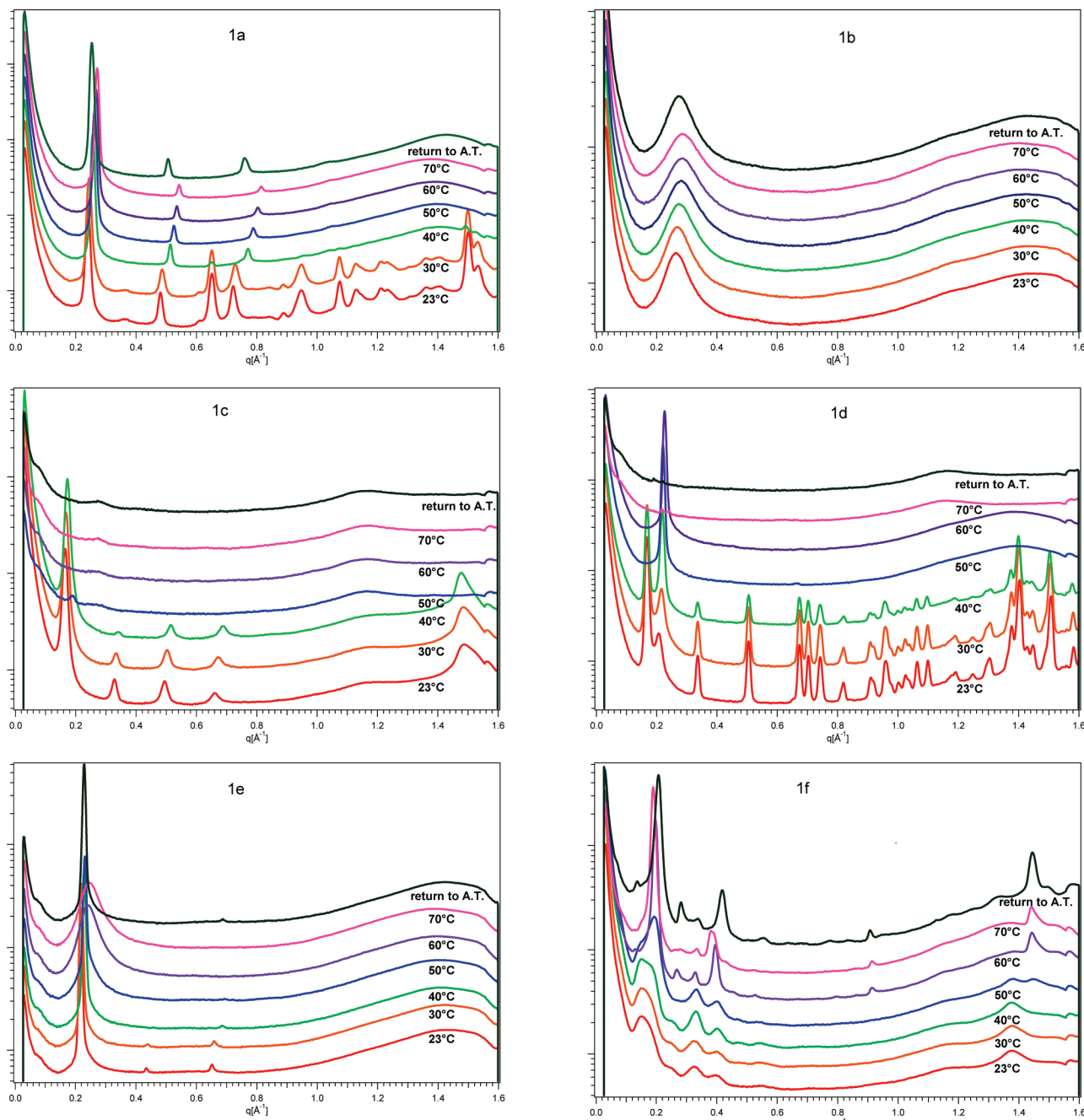


Figure 1. Temperature dependence of the SAXS/WAXS spectra of dry compounds: **1a**, C8C12; **1b**, C8C12X2; **1c**, C8C22; **1d**, C8C22X2; **1e**, C4C22X2; **1f**, C4C32X2.

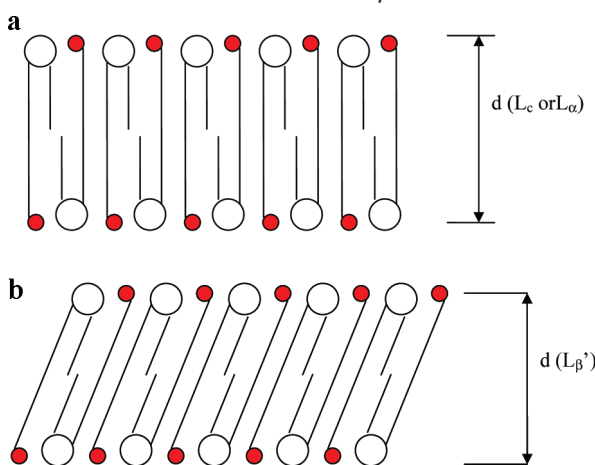
transforms into a lamellar L_α phase.⁶⁴ This state remains present even after cooling back to ambient temperature.

When the diacetylenic unit is introduced into the middle of the main hydrocarbon chain of the compound C8C22, we obtain an unsaturated, rigidified molecule C8C22X2. Indeed, as can be seen in the small angle and the wide angle X-ray scattering spectra in Figure 1d at 23 °C, the compound is in the well organized crystalline phase with the main peak at 0.168 \AA^{-1} that corresponds to the interlamellar distance of 37.4 \AA and two of its harmonics at 0.34 and 0.51 \AA^{-1} represent the pattern 1:2:3. There is a triplet structure starting at 0.67 \AA^{-1} that is a signature of a triple bond in this ordered liquid crystalline (L_c) alignment. There are many sharp peaks in the wide angle region confirming this assignment. However, the L_c phase is not the only phase present because we observe a peak next to the main peak at 0.206 \AA^{-1} ($d = 30.4 \text{ \AA}$) that evolves toward higher q

values by increasing the temperature. This peak corresponds to the lamellar L_α phase which coexists with the L_c phase up to 40 °C. At 50 °C, we observe only the L_α phase; there is no more liquid crystalline arrangement, since all of the typical peaks disappear in the wide angle region as observed for the compound C8C22 already at 50 °C. We assign the lamellar L_α structure on the basis of the present spectra even after cooling back to ambient temperature. The comparison with the saturated compound permits us to conclude that the $\pi-\pi$ stacking between the diacetylenic units is on the origin of keeping the ordered structure at higher temperatures than for the saturated compound.

In the following compound, C4C22X2, we have modified the hydrophilic/lipophilic balance by changing the number of methylene units in the side chain from eight to four units. The SAXS/WAXS spectra for this compound as a function of temperature are presented in Figure 1e. This temperature

SCHEME 2: (a) Symmetrical Ordering of Bolaamphiphile Molecules C8C12 for the L_α Phase or the L_c Phase; (b) Symmetrical Ordering of Bolaamphiphile Molecules C8C22 in the Lamellar $L_{\beta'}$ Phase



dependence is a very nice example of converting the lamellar L_α structure, which is present at lower temperatures, to the lamellar L structure which starts to appear around 50 °C. The L_α structure is a more ordered structure than L . The diffraction pattern with a main peak at 0.216 Å⁻¹ corresponds to an interlamellar distance of 29.1 Å. In addition, two of its harmonics appear at 0.43 and 0.66 Å⁻¹. In the wide angle region, one large peak and a complete absence of sharp peaks is observed, so we can conclude that the compound is in the lamellar L_α phase, and not in the crystalline L_c phase.

By increasing the temperature, the peaks shift toward wider angles which corresponds to shorter distances. This is explained as the increased fluidity of the hydrocarbon chains that favors the shortening of the interlamellar distance with increasing temperature. By continuing the increase of the temperature, the lamellar L_α layers can break, and the resulting structure is the lamellar L structure that contains parts of lamellae oriented randomly in different directions. The consequence is one broad peak in the small angle region which could be a result of polydisperse scattering on differently oriented lamellae in this isotropic lamellar L phase.

Further chemical modification that we introduced into this family of compounds is to increase the length of the main hydrocarbon chain to 32 methylenic units to obtain the compound C4C32X2. We observe the evolution of the SAXS/WAXS spectra as a function of temperature in the region between 23 and 70 °C in Figure 1f. At 23 °C, there is a series of peaks in the small angle region as well as in the wide angle region and we conclude to the lamellar crystalline structure, L_c . By increasing the temperature to 60 °C, a peak in the wide angle region, that has a form typical for the lamellar $L_{\beta'}$ phase, appears. Thus, for this compound, we assign the $L_{\beta'}$ lamellar phase at 60 and 70 °C. This phase remains present by returning back to ambient temperature. The diacetylenic unit in the middle of the long bridging hydrocarbon chain and the length of the chain are most probably on the origin of the organization of these molecules. Concerning Figure 1f, a more careful inspection brings us to the observation that the wider peak in the small angle region at 23 °C is most probably the superposition of the two peaks that come from the two possible orientations of the side chain with respect to the main bridging chain, as previously described for the molecule C8C22X2. Here, the short side chain most probably does not influence the $\pi-\pi$ stacking between

the diacetylenic units in the middle of the bridging chain of these molecules. By increasing the temperature, one of the molecular conformations becomes favored in comparison to the other—the one presented in Scheme 3b—and the interdigitated stacking of the molecules is obtained as they form the lamellar $L_{\beta'}$ structure detected from the presence of the typical peak in the wide angle region. In this phase $L_{\beta'}$, the interlamellar distance at 60 and 70 °C is 20.0 Å, while upon cooling to ambient temperature the phase changes to L_c and the interlamellar distance is 21.5 Å.

3.1.3. Analysis of the Compounds C8C12(aq), C8C12X2(aq), C8C22(aq), C8C22X2(aq), C4C22X2(aq), and C4C32X2(aq). For the compound **C8C12(aq)** of 8% in weight, we observe in Figure 2a a weak wide peak in the small angle region at 0.30 Å⁻¹ for the temperature range between 23 and 50 °C. At 60 °C, the intensity of this peak is decreased. We interpret it as an isotropic structure, I.

For the solution **C8C12X2(aq)** of 22% in weight, in Figure 2b, we observe one large peak in the small angle region that shifts toward wide angles (shorter distances) by increasing the temperature. Upon diluting, one can observe a large peak at 0.266 Å⁻¹ that shifts toward higher angles (shorter distances) by increasing the temperature to 70 °C (Table 2). The width of this peak is in accordance with the polydispersed signal coming from the isotropic structure in the solution. Thus, this phase is assigned as I (isotropic).

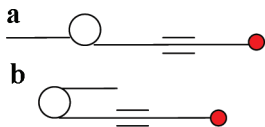
For the solution **C8C22(aq)** of 10% in weight, in Figure 2c, the typical peak for the $L_{\beta'}$ structure at 1.49 Å⁻¹ for 23 and 30 °C is observed. This structure is lost to the favor of isotropic I structure at higher temperatures, and upon cooling down back to ambient temperature, the compound adopts the $L_{\beta'}$ structure again.

The spectra of the **C8C22X2(aq)** compound of 6% in weight are presented in Figure 2d. Two peaks in the small angle region at 23 °C are observed: the one at 0.131 Å⁻¹ and another at 0.266 Å⁻¹ that remain present by heating the solution up to 30 °C. The first peak is the main peak, and the second peak is its first harmonic. Both peaks are a signature of a lamellar structure L_α because of the absence of sharp peaks in the wide angle region. By heating up the compound, a shoulder peak to the main peak appears at 40 °C that evolves toward 0.166 Å⁻¹ at 50 °C and 0.184 Å⁻¹ at 70 °C with two distinct values of 0.126 and 0.184 Å⁻¹. Cooling down to ambient temperature results in two peaks at 0.113 and 0.253 Å⁻¹ corresponding to interlamellar distances of 55.6 and 24.8 Å, that we interpret as the fluid lamellar structure L_α . The more careful inspection of Figure 2d brings us to the observation that by increasing the temperature the peaks in the small angle region not only shift toward wider angles (shorter distances) but also become wider. This can be connected to the formation of circular lamellar structures, such as vesicles, in this aqueous solution. Previously, we observed by TEM⁵¹ the formation of vesicles for these molecules in the diluted aqueous media which corroborates the observation obtained by the inspection of the SAXS/WAXS measurements.

In Figure 2e, the series of spectra for the aqueous solution of the compound **C4C22X2(aq)** of 15% in weight as a function of temperature is shown. At 23 °C, the main peak at 0.179 Å⁻¹ that corresponds to a distance of 35.1 Å and its first harmonic at 0.36 Å⁻¹ are present. In the wide angle region, one broad peak can be observed and the absence of the sharp peaks helps us to assign the fluid lamellar phase, L_α . By heating the sample, the main peak shifts toward wider angles and the variation of the interlamellar distance with the temperature is around 15% due to the increased fluidity and thus flexibility of the

TABLE 1: Temperature Dependence of Interlamellar Distances as Well as the Phase Assignment for the Dry Compounds C8C12(dry), C8C12X2(dry), C8C22(dry), C8C22X2(dry), C4C22X2(dry), and C4C32X2(dry)

T/°C	C8C12(dry), 1a		C8C12X2(dry), 1b		C8C22(dry), 1c		C8C22X2(dry), 1d		C4C22X2(dry), 1e		C4C32X2(dry), 1f	
	d/Å	phase	d/Å	phase	d/Å	phase	d/Å	phase	d/Å	phase	d/Å	phase
23	26.2	L _c	23.8	L	38.1	L _{β'}	37.4	L _c	29.1	L _α		L _c
30	25.8	L _c	23.4	L	37.4	L _{β'}	30.4	L _α				
40	24.6	L _α	22.8	L	36.5	L _{β'}	37.4	L _c	28.7	L _α		L _c
50	24.0	L _α	22.4	L		L _α	27.4	L _α	27.2	L _α		L _c
60	23.5	L _α	22.1	L		L _α	27.7	L _α	26.0	L	31.4	L _{β'}
70	23.2	L _α	22.0	L		L _α		L _α	25.5	L	31.4	L _{β'}
23	26.2	L _α	24.1	L		L _α		L _α	27.4	L _α	29.2	L _c

SCHEME 3: (a) Bolaamphiphile Molecule in Extended Chain Position; (b) Bolaamphiphile Molecule in Parallel Chain Arrangement

hydrocarbon chains. By cooling back down to ambient temperature, one observes the main peak with its first and second harmonics, typical of the fluid lamellar structure L_α.

Finally, in the series of spectra shown in Figure 2f, the aqueous solution of the compound **C4C32X2(aq)** of 10% in weight has been studied as a function of temperature. One can observe a large peak at 0.145 Å⁻¹ and another large peak at 0.364 Å⁻¹. We can fit a sinus function between the two maxima of those two peaks. In the literature,^{7,47,65} mostly the lyotropic systems have been studied, and for such systems, the observation of the peaks at very small angles (VSAXS) in a harmonic repetition is a signature for the individual bilayers that can be compatible with nanotubular structures.⁶⁴ We have previously observed by TEM⁵¹ and FFEM that this molecule in aqueous solutions gives filaments probably corresponding to nanotubes. In the literature, the thorough discussion of the nanotubes that may have variable diameter or different tilts has been reported.⁶⁶

The interlamellar distances and their evolution as a function of temperature for dry compounds have been reported in Table 1 and for the aqueous solutions in Table 2. In Figure 3a, the temperature dependence of the interlamellar distances for dry compounds is given. We observe the general tendency of decreasing the interlayer distance by increasing the temperature which is interpreted as an increase of the fluidity of molecular chains. In Figure 3b, the variation of the interlamellar distances for aqueous solutions discussed previously is shown. The interlamellar distance is about 12 Å larger for C4C22X2 than for C8C12X2, and for C4C32X2, it is about 24 Å larger than for C8C12X2, so we conclude that the molecules are in their stretched shape. The decrease in the interlamellar distances is about 8% for C8C12X2, 15% for C4C22X2, and 14% for C4C32X2 between 23 and 70 °C.

Figure 4a and b represent the evolution of supramolecular assemblies as a function of temperature for all of the bolaamphiphile molecules discussed previously for dry compounds and for aqueous solutions, respectively.

3.2. Polarized Optical Microscopy. Identification of the lyotropic mesophases of bolaamphiphiles has been carried out also by polarized optical microscopy on cooling from the isotropic liquid (short preheating). The contact preparations

between bipolar lipids C8C22X2, C8C12X2, C8C12, and C8C32X2 and water reveal myelins and maltese crosses (Figures 5, 1–3) which is indicative of the presence of lamellar phases and large multilamellar vesicles.⁶⁷ Unlike the C₁₂- and C₂₂-type bolaamphiphiles, bolalipid C4C32X2 with a C₃₂ polymethylene chain afforded fibrous filaments with widths of several nanometers (Figure 5, 4). This structure suggests a different way of self-organization, other than vesicular, for the relatively highly concentrated domain which is in accordance with the SAXS/WAXS observations described above and the interpretation of the structure as nanotubes.

4. Discussion

This work deals with the investigation of the self-assembling properties of unsymmetrical bolaamphiphile lipids bearing one sugar polar headgroup based on D-glucuronolactone issued from the primary resources (wheat) and one glycine betaine (sugar beet) polar headgroup. There are two hydrocarbon chains attached to the sugar unit: one main chain that interconnects the two polar headgroups and one side chain that is attached to the anomeric position of the sugar ring as presented in Scheme 1. The length of the main (bridging) chain has been modified, and this structure has been compared to the saturated compounds with 12 and 22 methylene units (C8C12 and C8C22). In order to rigidify the bridging chain, we have introduced a diacetylenic unit in the middle of the chain and thus synthesized the compounds C8C12X2 and C8C22X2. For the purpose of modifying the hydrophilic/lipophilic balance, the chain at the anomeric position has been shortened for four methylene units and the compounds C4C22X2 and C4C32X2 have been obtained. The results of our measurements of small angle and wide angle X-ray scattering bring us to the conclusion that each chemical modification affects substantially the self-organizing patterns of these molecules. Thus, for C8C12, we observe the crystalline lamellar (L_c) phase at temperatures of 23 and 30 °C, while in the temperature interval between 40 and 70 °C the same bolaamphiphile molecules adopt the lamellar L_α organization (Scheme 2a).

The saturated molecules with longer bridging chain C8C22 are organized differently and at 23 °C they form the tilted lamellar phase L_{β'} (Scheme 2b). The phase L_{β'} is conserved up to 40 °C, while from 50 to 70 °C these molecules form the fluid lamellar phase.

With the aim to rigidify the bridging chain, a diacetylenic unit has been incorporated in the middle of the chain to obtain the compounds C8C12X2 and C8C22X2. Comparing the saturated compound C8C12 with the unsaturated compound C8C12X2, we can observe that the saturated compound adopts

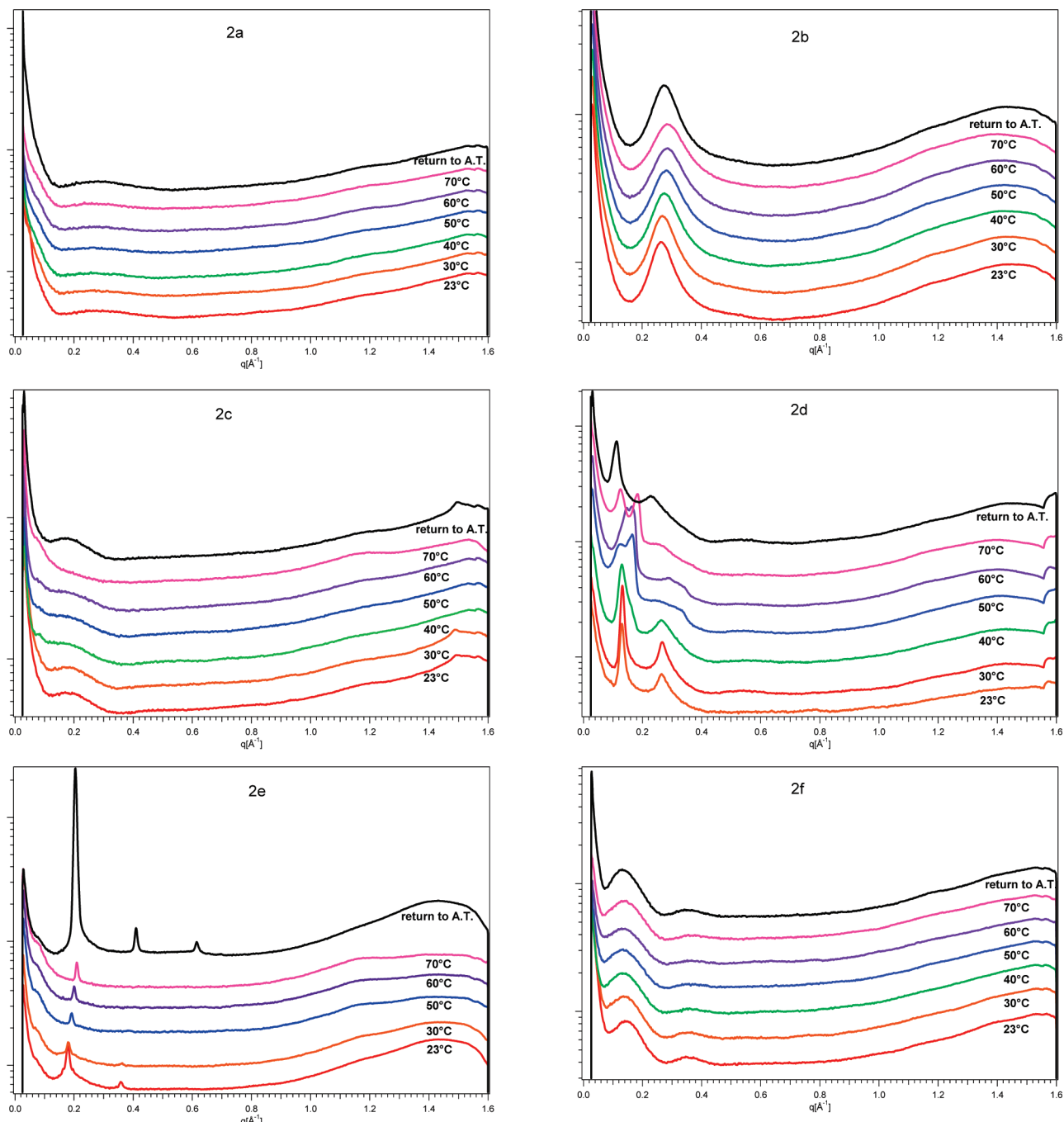


Figure 2. Temperature dependence of the spectra of aqueous solutions of the bolaamphiphiles: **2a**, C8C12(aq); **2b**, C8C12X2(aq); **2c**, C8C22(aq); **2d**, C8C22X2(aq); **2e**, C4C22X2(aq); **2f**, C4C32X2(aq).

TABLE 2: Temperature Dependence of Interlamellar Distances as Well as the Phase Assignment for the Hydrated Compounds C8C12(aq), C8C12X2(aq), C8C22(aq), C8C22X2(aq), C4C22X2(aq), and C4C32X2(aq)

T/°C	C8C12(aq), 2a		C8C12X2(aq), 2b		C8C22(aq), 2c		C8C22X2(aq), 2d		C4C22X2(aq), 2e		C4C32X2(aq), 2f	
	phase	d/Å	phase	d/Å	phase	d/Å	phase	d/Å	phase	d/Å	phase	d/Å
23	I	23.6	I	—	L _{β'}	—	L _α	35.1	L _α	47.6	nanotubes	—
30	I	23.3	I	—	L _{β'}	—	L _α	34.9	L _α	47.6	nanotubes	—
40	I	22.8	I	—	I	—	L _α	—	—	46.2	nanotubes	—
50	I	22.2	I	—	I	—	I	32.9	L _α	45.9	nanotubes	—
60	I	22.0	I	—	I	—	I	31.4	L _α	45.2	nanotubes	—
70	I	21.8	I	—	I	—	I	29.9	L _α	44.6	nanotubes	—
23	I	22.8	I	—	L _{β'}	—	L _α	31.4	L _α	46.5	nanotubes	—

a lamellar crystalline L_c phase at lower temperatures and the lamellar L_α phase in the temperature interval between 40 and 70 °C. In contrast to this supramolecular structure, the unsatur-

ated compound C8C12X2 is present in the lamellar L phase in the whole temperature interval measured from 23 °C up to 70 °C. This means that for this molecule the longer lamellae are

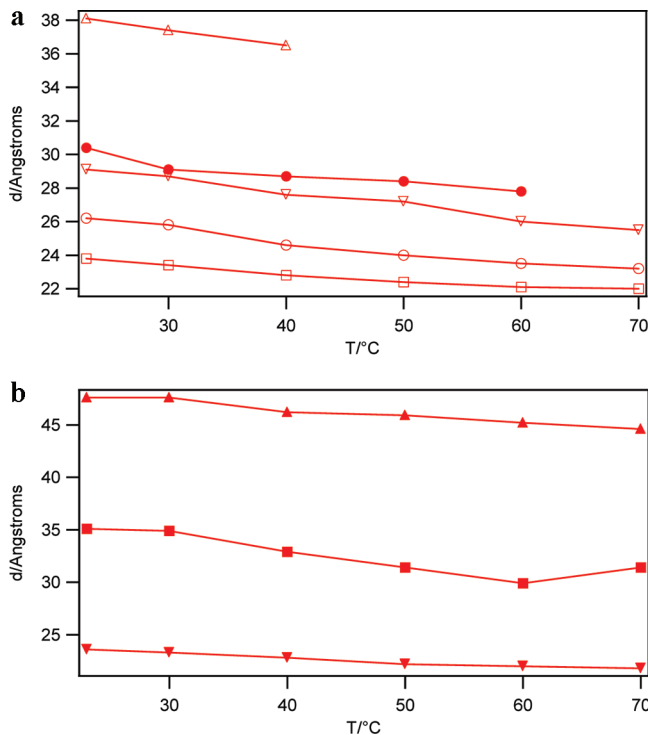


Figure 3. (a) Interlayer distances of the compounds C8C12 (○), C8C12X2 (□), C8C22 (△), C8C22X2 (●), and C4C22X2 (▽). (b) The shift of the interlamellar distances of the aqueous solutions of the compounds C8C12X2 (▼), C4C22X2 (■), and C4C32X2 (▲).

not present but we observe the smaller segments which are distributed in an isotropic way and form a lamellar L phase.

The saturated compound with 22 methylene units in the main bridging chain, C8C22, is in the tilted lamellar phase L'_β from 23 to 40 °C, and for higher temperatures, the spectra reveal the lamellar structure L_α . The unsaturated analogue is C8C22X2. This compound organizes in the crystalline lamellar phase for the temperature range between 23 and 40 °C. For temperatures higher than 50 °C, the phase is fluid lamellar. We can see on the example of these two couples of saturated and unsaturated compounds that the increase in temperature results in less ordered supramolecular structures, for saturated compounds. For the unsaturated compounds, we observe that the compound with the longer bridging chain at the ambient temperature adopts a crystalline lamellar structure, while the compound with the shorter bridging chain is in a less organized structure. We can explain this by the influence of the side chain. While for the compound C8C12X2 the side chain can shield the diacetylenic unit in the main chain, in the compound C8C22X2, the diacetylenic units are free to organize and can stack, thus providing the crystalline L_c structure for 23–40 °C.

We have studied the influence of the length of the side chain by observing the self-organizing properties of the molecule C4C22X2 compared to the molecule C8C22X2, both in the dry state. The compound C4C22X2 is in the fluid lamellar phase in the temperature interval between 23 and 40 °C, and for temperatures above 50 °C, it adopts a lamellar L phase. The ordering in this compound is less pronounced than in C8C22X2 where we observed the crystalline lamellar phase for the temperature interval between 23 and 40 °C. We can conclude that the side chain length has its influence for ordering the bolaamphiphile molecules. The phenomenon of packing states of a homologous series of mixed-chain phosphatidylcholines has been thoroughly studied in the literature by a molecular

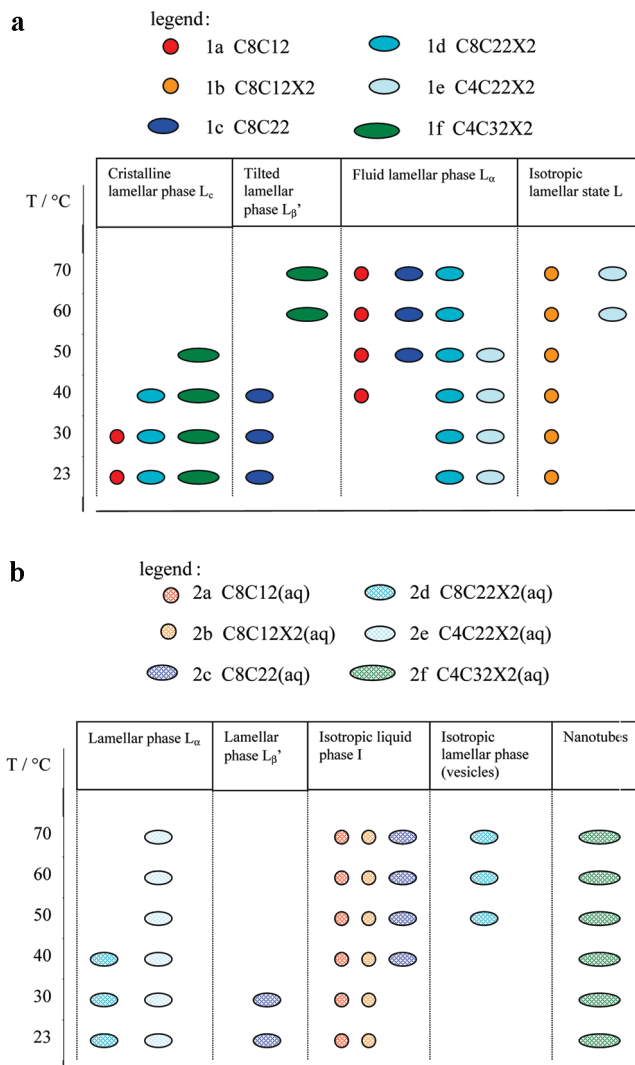


Figure 4. (a) Phase diagram of dry bolaamphiphiles as a function of the temperature and the evolution of their supramolecular structures. (b) Phase diagram of aqueous solutions of bolaamphiphiles as a function of the temperature and the evolution of their supramolecular structures.

mechanics study⁶⁸ as well as the packing in mixed-chain phospholipids and interdigitated bilayer systems.⁶⁹

From the values for the lamellar distances for C8C12 (Table 1), we can deduce that the bolaamphiphile molecules are stretched and most probably aligned in the symmetrical pattern,^{65,66} as shown in Scheme 2a. Upon heating, the chains become more fluid, so the polar heads are nearer to each other in the L_α phase. Upon hydrating the initially dry phase, the polar heads become surrounded by the water molecules which results in the “swelling” of the system.

For the molecule C8C22 that contains a longer main hydrocarbon chain of 22 methylene units, the situation is similar and molecules are in their stretched conformation and present the tilted lamellar phase L'_β . Upon heating, these molecules adopt the lamellar L_α structure with more flexibility of the hydrocarbon chains and the distance between the polar heads becomes shorter.

The compounds that contain the triple bond in the middle of the bridging hydrocarbon chain can adopt the conformation where the side chain is on the opposite side of the polar head compared to the main chain, as schematically presented in Scheme 3a. In this way, the ordering of the triple bonds is

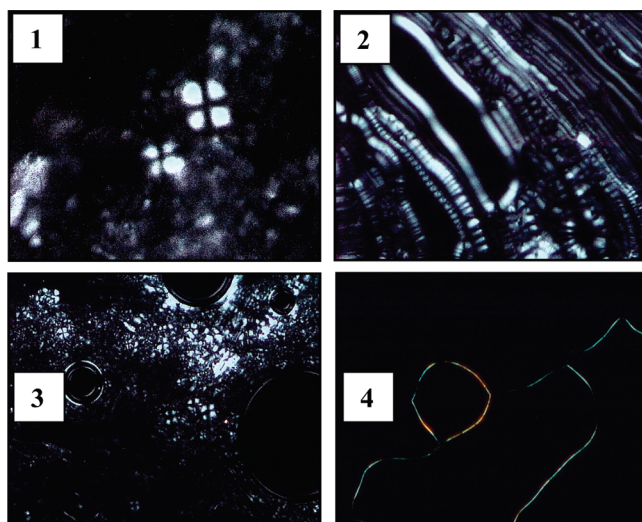


Figure 5. Room temperature photomicrographs of maltese crosses (1 and 3) and myelinins (2) observed for bipolar lipids (1) C8C22X2 (d), (2) C8C12X2 (b), and (3) C8C12 (a) and thin filaments (4) for bolaamphiphile C8C32X2 (f) ($\times 10$).

enabled. This can in particular be analyzed by looking at Figure 1d which corresponds to SAXS/WAXS spectra of the dry compound C8C22X2. There are two peaks in the small angle region, one at $q = 0.18 \text{ \AA}^{-1}$ and the other at 0.21 \AA^{-1} for this liquid crystalline phase at 23°C . We interpret it as the coexistence of the two phases where the first peak ($d = 37.4 \text{ \AA}$) corresponds to the alignment of molecules stretched in a manner presented in Scheme 3a, and the second peak ($d = 30.4 \text{ \AA}$) corresponds to the molecules represented by Scheme 3b. By heating up, the structure of Scheme 3a is lost to the profit of the conformation where two hydrocarbon chains are disposed one parallel to the other, as presented in Scheme 3b. The

conformation presented in Scheme 3a is not hydrated because of the stretched side hydrocarbon chain that is hydrophobic. The triplet between 0.6 and 0.8 \AA^{-1} is the signature of a triple bond, and we deduce that in the crystalline L_c phase the alignment between the chains containing the triple bond is favored by stacking the molecules.

It is important to stress that it is the length of the longer bridging hydrocarbon chain that fixes the lamellar distance. The molecules are in their transmembrane position stretched and aligned most probably in a symmetrical manner.

The compound with 32 methylenic units in the main bridging hydrocarbon chain, C4C32X2, is in the lamellar crystalline phase, L_c , in the temperature interval between 23 and 50°C , while from 60 to 70°C it adopts a tilted lamellar L_β' phase. We observe the influence of the increasing temperature on decreasing the structural order being in accordance with the increased entropy of the system.

The compound C8C32X2 in the aqueous solution is specific, compared to the other five compounds, because it shows a filamentary structure observed under polarization microscope that we interpret as the nanotubular structure in aqueous solution. This observation is coherent with the previous results of the cryo-TEM measurements⁵¹ that indicated a filamentary network in aqueous solutions. Compared to the optical polarization microscopy measurements, we can conclude that this compound organizes as nanotubes in aqueous solutions.

One point that should be discussed as well is the thermodynamic stability of different phases. This addresses a major scientific problem concerning the stability/instability of the phases as a function of the temperature in time. We have performed an experiment on one of our bolaamphiphile molecules ($e = \text{C4C22X2 (dry)}$) by heating it up to 70°C and then cooling it back down to 23°C . Then, we collected the spectra every 2 h for 12 h. These spectra were all the same, as shown

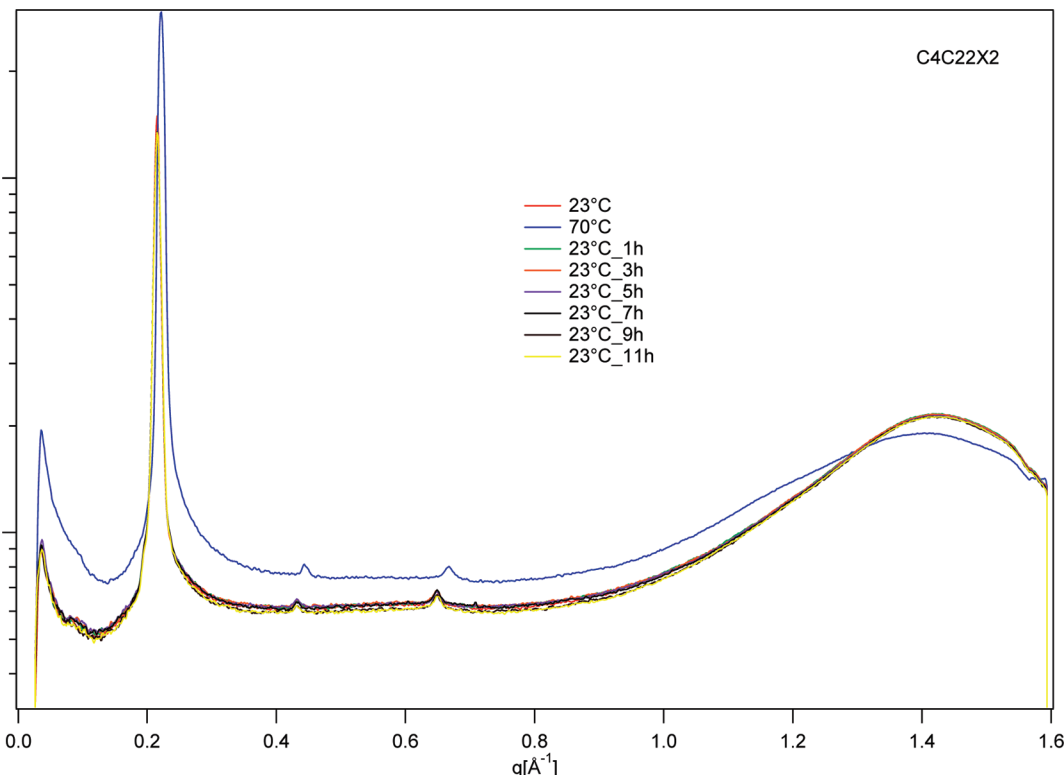


Figure 6. Spectra of bolaamphiphile molecule C4C22X2 (e) in its dry state at 23°C before heating to 70°C and after cooling back down to 23°C . Spectra were taken every 2 h for a 12 h period, and they are superposed one to another.

TABLE 3: Phases at 23 °C before and after Heating the Sample to 70 °C

		23 °C before heating	23 °C after heating
1a	C8C12(dry)	L _c	L _α
1b	C8C12X2(dry)	L	L
1c	C8C22(dry)	L _{β'}	L _α
1d	C8C22X2(dry)	L _c	L _α
1e	C4C22X2(dry)	L _α	L _α
1f	C4C32X2(dry)	L _c	L _c
2a	C8C12(aq)	I	I
2b	C8C12X2(aq)	I	I
2c	C8C22(aq)	L _{β'}	L _{β'}
2d	C8C22X2(aq)	L _α	L _α
2e	C4C22X2(aq)	L _α	L _α
2f	C4C32X2(aq)	nanotubes	nanotubes

in Figure 6, so we conclude that there is no thermal degradation of the sample and the sample is in its thermal and thermodynamic equilibrium. We wish to inspect this point as a future work for all of the compounds, because for some of the compounds the initial and the final room temperature phases are not equivalent. If we analyze the behavior of different molecules prior to heating and after heating, we obtain the results listed in Table 3.

The differences between the initial room temperature phase before heating and the final room temperature phase after heating are present in the dry state in two saturated compounds, C8C12 and C8C22, as well as for two unsaturated compounds, C8C22X2 and C4C32X2. It should be noted that all of the spectra in this work have been taken for the thermally equilibrated compounds for 1 h. The polymorphism control has been studied by X-ray diffraction and by calorimetry coupling on solid lipid nanoparticles based on trilaurin mixed with 4% of cholesterol and four polymorphic forms were identified.⁷⁰ Another important work related to our study concerns the structure and polymorphism of bipolar isopranyl ether lipids from archaeabacteria.³⁹ In this paper, four lipid preparations were studied; the total and polar lipid extracts, and two hydrolytic fractions, the symmetric glycerol dialkyl glycerol tetraether and the asymmetric glycerol dialkyl nonitol tetraether, as a function of water content and temperature, using X-ray scattering techniques. However, these systems are mixed systems, while in our work we present the studies of pure synthesized molecules. In the cited ref 39, two cubic phases are observed in the total and polar lipid extracts, which display a remarkable degree of metastability, most unusual in lipid phase transitions involving structures with chains in the α conformation. The authors explain this phenomenon by the interplay of the physical structure of the cubic phases and the chemical structure of the lipid molecules. The possibility is discussed that this polymorphism reflects a fundamental property of lipids, closely related to their physiological role.

5. Conclusion

In conclusion, each chemical modification affects substantially the self-organizing properties of the molecules in dry compounds as well as in the aqueous solutions. The molecules studied in this work show thermotropic and lyotropic behavior. They self-organize in a wide panel of supramolecular organizations, the lamellar phases L, L_α, L_{β'}, L_c, the isotropic liquid phase I, as well as the nanotubes.

The entropy of these systems increases with the increased temperature which is in accordance with less and less ordered supramolecular structures as a function of increasing temperature. In the case where one structure is preserved over a

temperature interval (for example L_α), the fluidity of the hydrocarbon chains is increased by elevated temperature corresponding to shorter interlamellar distances and higher entropy.

The applications of these molecules are still under investigation, but as they form lamellar structures, their application field may be very wide. The property of these molecules to organize in aqueous solutions as the lamellar structures that mimic membranes, quite stable in the range of temperatures between 23 and 70 °C in most of the cases is *a priori* interesting for pharmacological or cosmetic applications. Our future aim is to investigate the fluidity of these membranes as well as their permeability. Having this aim in sight, we have previously synthesized the spin labeled analogue of the molecule C8C12 in order to follow the transversal rotation movement or *flip-flop*.⁷¹

Acknowledgment. M.B. is grateful to the French Ministry of Research and Education for the Ph.D. grant. We thank Marko Jeftić for the proofreading of the manuscript. The French Ministry of Research and Education and CNRS are gratefully acknowledged for financial support.

References and Notes

- (1) Lindner, P.; Zemb, Th. *Neutrons, X-Rays and Light. Scattering Methods Applied to Soft Condensed Matter*; Elsevier: Paris, 2002.
- (2) Ryan, A. J. Chapter 18 in ref 1, pp 441–446.
- (3) Pedersen, J. S. Chapter 6 in ref 1, pp 127–144.
- (4) Rieger, J. Chapter 21 in ref 1, pp 515–531.
- (5) May, R. P. Chapter 19 in ref 1, pp 463–480.
- (6) Lecolinet, G.; Gulik, A.; Mackenzie, G.; Goodby, J. W.; Benvegnu, T. *Chem.—Eur. J.* **2002**, *8*/3, 585–593.
- (7) Valéry, C.; Artzner, F.; Robert, B.; Gulick, T.; Keller, G.; Grabielle-Madelmont, C.; Torres, M.-L.; Cherif-Cheikh, R.; Paternostre, M. *Biophys. J.* **2004**, *86*, 2484–2501.
- (8) Van Grondelle, W.; López Iglesias, C.; Coll, E.; Artzner, F.; Paternostre, M.; Lacombe, F.; Cardus, M.; Martínez, G.; Montez, M.; Cherif-Cheikh, R.; Valéry, C. *J. Struct. Biol.* **2007**, *160*, 211–223.
- (9) Mannock, D. A.; Collins, M. D.; Kreichbaum, M.; Harper, P. E.; Gruner, S. M.; Elhaney, R. N. *Chem. Phys. Lipids* **2007**, *148*, 26–50.
- (10) Harms, M.; Mackeben, S.; Müller-Goymann, C. C. *Colloids Surf., A* **2005**, *259*, 81–87.
- (11) Hyde, S. T. *Curr. Opin. Solid State Mater. Sci.* **1996**, *1*, 653–662. Tresset, G. *PMC Biophys.* **2009**, *2*/3, 1–22.
- (12) Seddon, J. M. *Curr. Opin. Colloid Interface Sci.* **2001**, *6*, 242–243.
- (13) Squires, A. M.; Templer, R. H.; Seddon, J. M.; Woenckhaus, J.; Winter, R.; Finet, S.; Theyencheri, N. *Langmuir* **2002**, *18*, 7384–7392.
- (14) Larsson, K. *Curr. Opin. Colloid Interface Sci.* **2000**, *4*, 449–456.
- (15) Almgren, M.; Edwards, K.; Karlsson, G. *Colloids Surf., A* **2000**, *174*, 3–21.
- (16) Luzatti, V.; Vargas, R.; Mariani, P.; Gulik, A.; Delacroix, H. J. *Mol. Biol.* **1993**, *229*, 540–551.
- (17) De Campo, L.; Yaghmur, A.; Sagalowicz, L.; Leser, M. E.; Watzke, H.; Glatter, O. *Langmuir* **2004**, *20*, 5254–5261.
- (18) Drummond, C.; Fong, C. *Curr. Opin. Colloid Interface Sci.* **2000**, *4*, 449–456.
- (19) Larsson, K. *J. Phys. Chem.* **1989**, *93*, 7304–7314.
- (20) Boyd, B. J. *Int. J. Pharm.* **2003**, *260*, 239–247.
- (21) Vauthay, S.; Milo, Ch.; Frossard, Ph.; Garti, N.; Leser, M. E.; Watzke, H. J. *J. Agric. Food Chem.* **2000**, *48*, 4808–4816.
- (22) Caboi, F.; Nylander, T.; Razumas, V.; Talaikyte, Z.; Monduzzi, M.; Larsson, K. *Langmuir* **1997**, *13*, 5476–5483.
- (23) Masum, S. M.; Li, S. J.; Tamba, Y.; Yamashita, Y.; Tanaka, T.; Yamazaki, M. *Langmuir* **2003**, *19*, 4745–4753.
- (24) Nylander, T.; Mattisson, C.; Razumas, V.; Miezis, Y.; Häkansson, B. *Colloids Surf., A* **1996**, *114*, 311–320.
- (25) Landau, E. M.; Rummel, G.; Rosenbusch, J. P.; Cowan-Jacob, S. W. *J. Phys. Chem. B* **1997**, *101*, 1935–1937.
- (26) Caffrey, M. *Curr. Opin. Struct. Biol.* **2000**, *10*, 486–497.
- (27) Caffrey, M. *J. Struct. Biol.* **2003**, *142*, 108–132.
- (28) Briggs, J.; Chung, H.; Caffrey, M. *J. Phys. II* **1996**, *6*, 723–751.
- (29) Qiu, H.; Caffrey, M. *J. Phys. Chem. B* **1998**, *102*, 4819–4829.
- (30) Qiu, H.; Caffrey, M. *Chem. Phys. Lipids* **1999**, *100*, 55–79.
- (31) Qiu, H.; Caffrey, M. *Biomaterials* **2000**, *21*, 223–234.
- (32) Mannock, D. A.; McElhaney, R. N.; Harper, P. E.; Gruner, S. M. *Biophys. J.* **1994**, *66*, 734–740.

- (33) Lewis, R. N. A. H.; McElhaney, R. N.; Österberg, F.; Gruner, S. M. *Biophys. J.* **1994**, *66*, 207–216.
- (34) Mannock, D. A.; McElhaney, R. N. *Biochem. Cell Biol.* **1991**, *69*, 863–867.
- (35) Kuttenreich, H.; Hinz, H. J.; Inczedy-Marcsek, M.; Koynova, R.; Tenchov, B.; Laggner, P. *Chem. Phys. Lipids* **1988**, *47* (4), 245–260.
- (36) Fuhrhop, J. H.; Wang, T. *Chem. Rev.* **2004**, *104*, 2901–2937. Abbel, R.; van der Weegen, R.; Meijer, E. W.; Schenning, A. P. H. J. *Chem. Commun.* **2009**, *1697*, 1699.
- (37) Benvegnu, T.; Brard, M.; Rethore, G.; Plusquellec, D. *Cahiers de Formulation “Formulations cosmétique: Matières premières, concepts et procédés innovants”*, *EDP Sciences* **2005**, *12*, 66–81.
- (38) Benvegnu, T.; Rethore, G.; Brard, M.; Richter, W.; Plusquellec, D. *Chem. Commun.* **2005**, *44*, 5536–5538.
- (39) Gulik, A.; Luzzati, V.; De Rosa, M.; Gambacorta, A. *J. Mol. Biol.* **1985**, *182*, 131–149.
- (40) Gulik, A.; Luzzati, V.; De Rosa, M.; Gambacorta, A. *J. Mol. Biol.* **1988**, *201*, 429–435.
- (41) Luzzati, V.; Gambacorta, A.; De Rosa, M.; Gulik, A. *Annu. Rev. Biophys. Biophys. Chem.* **1987**, *16*, 25–47.
- (42) Benvegnu, T.; Lemière, L.; Cammas-Marion, S. *Eur. J. Org. Chem.* **2008**, *4725*–4744.
- (43) Gambacorta, A.; Gliozi, A.; DeRosa, M. *World J. Microbiol. Biotechnol.* **1995**, *11*, 115–131.
- (44) Menger, F. M.; Chen, X. Y.; Broccolini, S.; Hopkins, H. P.; Hamilton, D. *J. Am. Chem. Soc.* **1993**, *115*, 6600–6608.
- (45) Shimizu, T.; Iwaura, R.; Masuda, M.; Hanada, T.; Yase, K. *J. Am. Chem. Soc.* **2001**, *123*, 5947–5955.
- (46) Shimizu, T.; Masuda, M. *J. Am. Chem. Soc.* **1997**, *119*, 2812–2818.
- (47) Ambrosi, M.; Fratini, E.; Alfredsson, V.; Ninham, B. W.; Giorgi, R.; LoNstro, P.; Baglioni, P. *J. Am. Chem. Soc.* **2006**, *128*, 7209–7214.
- (48) Hau, F.; He, X.; Huang, J.; Li, Z.; Wang, Y.; Fu, H. *J. Phys. Chem. B* **2004**, *108*, 5256–5262.
- (49) Shimizu, T.; Masuda, M.; Minamikawa, H. *Chem. Rev.* **2005**, *105*, 1401–1443.
- (50) Meister, A.; Drescher, S.; Garamus, V.; Karlsson, G.; Graf, G.; Dobner, B.; Blume, A. *Langmuir* **2008**, *24*, 6238–6246.
- (51) Berchel, M.; Lemière, L.; Trépout, S.; Lambert, O.; Jeftić, J.; Benvegnu, T. *Tetrahedron Lett.* **2008**, *49*, 7419–7422.
- (52) Guilbot, J.; Benvegnu, T.; Legros, N.; Plusquellec, D.; Dedieu, J. C.; Gulik, A. *Langmuir* **2001**, *17*, 613–618.
- (53) Roessle, M.; Manakova, E.; Lauer, I.; Nawroth, T.; Holzinger, J.; Narayanan, T.; Bernstorff, S.; Amenitsch, H.; Heuman, H. *J. Appl. Crystallogr.* **2000**, *33*, 548–551.
- (54) Macanlay, S. R. *J. Org. Chem.* **1980**, *45*, 734–735.
- (55) Kucerka, N.; Pencer, J.; Sachs, J. N.; Nagle, J. F.; Katsaras, J. *Langmuir* **2007**, *23*, 1292–1299.
- (56) Koynova, R.; Caffrey, M. *Biochim. Biophys. Acta* **1998**, *1376*, 91–145.
- (57) Zemb, Th.; Dubois, M.; Demé, B.; Gulik-Krywicki, Th. *Science* **1999**, *283*, 816–819.
- (58) Shimizu, T.; Masuda, M.; Minamikawa, H. *Chem. Rev.* **2005**, *105*, 1401–1443.
- (59) Shimizu, T. *J. Polym. Sci., Part A: Polym. Chem.* **2008**, *46*, 2601–2611.
- (60) Brazhnik, K. P.; Vreeland, W. N.; Hutchinson, J. B.; Kishore, R.; Wells, J.; Helmerson, K.; Locascio, L. E. *Langmuir* **2005**, *21*, 10814–10817.
- (61) Hauet, N.; Artzner, F.; Boucher, F.; Grabielle-Madelmont, C.; Cloutier, I.; Keller, G.; Lesieur, P.; Durand, D.; Paternostre, M. *Biophys. J.* **2003**, *84*, 3123–3137.
- (62) Zantl, R.; Artzner, F.; Rapp, G.; Rädler, J. O. *Europhys. Lett.* **1998**, *45*, 90–96.
- (63) Artzner, F.; Zantl, R.; Rapp, G.; Rädler, J. O. *Phys. Rev. Lett.* **1998**, *81*, 5015–5018.
- (64) Thomas, B. N.; Safinya, C. R.; Plano, R. J.; Clark, N. A. *Science* **1995**, *267*, 1635–1638.
- (65) Goodby, J. W.; Götz, V.; Cowling, S. J.; Mackenzie, G.; Martin, P.; Plusquellec, D.; Benvegnu, T.; Boullanger, P.; Lafont, D.; Queneau, Y.; Chambert, S.; Fitremann, J. *Chem. Soc. Rev.* **2007**, *36*, 1971–2032.
- (66) Oda, R.; Artzner, F.; Laguerre, M.; Huc, I. *J. Am. Chem. Soc.* **2008**, *130* (44), 14705–14712.
- (67) van Hal, D. A.; Bouwstra, J. A.; van Rensen, A.; Jeremiassie, E.; de Vringer, T.; Junginger, H. E. *J. Colloid Interface Sci.* **1996**, *178*, 263–273.
- (68) Li, S.; Wang, Z. Q.; Lin, H. N.; Huang, C. *Biophys. J.* **1993**, *65*, 1415–1428.
- (69) Huang, C. *Klin Wochenschr.* **1990**, *68*, 149–165.
- (70) Allais, C.; Keller, G.; Lesieur, P.; Ollivon, M.; Artzner, F. *J. Therm. Anal. Calorim.* **2003**, *74*, 723–728.
- (71) Berchel, M.; Lemière, L.; Jeftić, J.; Benvegnu, T. *Tetrahedron Lett.* **2008**, *49*, 4690–4692.

JP905747R